Original Paper

Skin Pharmacology and Physiology

Skin Pharmacol Physiol 2014;27:263–275
DOI: 10.1159/000358272

Received: August 5, 2013
Accepted after revision: December 30, 2013
Published online: June 13, 2014

Dermal Xenobiotic Metabolism: A Comparison between Native Human Skin, Four in vitro Skin Test Systems and a Liver System

Christian Wiegand[a] Nicola J. Hewitt[b] Hans F. Merk[c] Kerstin Reisinger[a]

[a]Henkel AG & Co. KGaA, Düsseldorf, [b]Erzhausen, and [c]Department of Dermatology, University Hospital, RWTH Aachen, Aachen, Germany

Key Words

Xenobiotic metabolism · Skin · Phenion® Full-Thickness Skin Model · Open-Source Reconstructed Epidermis model

Abstract

The xenobiotic metabolism of 4 in vitro human skin test systems (2D and 3D) was compared with that of the native human skin samples from which the skin test systems had been produced. In total 3 skin samples were investigated, each from a different donor to exclude variability due to gender, donor or tissue supplier. In addition, the skin cultures were compared with a surrogate of the liver. Basal and induced phase I and phase II enzymes were analyzed regarding gene/protein expression as well as enzyme activity. The distinctions between the different test systems and the two dermal compartments (epidermis and dermis) were more noticeable than any donor variability. The 3D models of skin and liver mirrored the in vivo situation more realistically than did the monolayer cultures. Phase I metabolism was more pronounced in the hepatic model, whereas phase II metabolism was more prominent in the reconstructed skin. These results show that reconstructed skin models are a valuable tool for organ-specific safety assessment with regard to xenobiotic metabolism.

Introduction

The skin is the largest organ of the human body and the first site of contact for many external stimuli. It protects the body in several ways, and its barrier function determines the local and systemic bioavailability of dermally applied substances, which may be present in high concentrations. Previously, the skin has been described only as a physical permeability barrier. However, today it is well known that skin also has the capacity to metabolize xenobiotics [1, 2].

In addition to monolayer cultures of keratinocytes or fibroblasts, reconstructed human skin equivalents have gained importance as an animal-free alternative to assess toxicological effects relevant to humans and the efficacy of raw materials, cosmetics, pharmaceuticals, biocides and agrochemicals [3–5]. This is especially relevant with respect to the already existing implementation of the 7th Amendment to the EU Cosmetic Directive [6], which bans animal tests for compounds which are used in cosmetic products, and the Registration Evaluation and Authorisation of Chemicals (REACh) regulations [7], which require the avoidance of animal tests and the use of methods relevant to humans. Consequently, growing efforts are being put into assays using in vitro models which mir-

KARGER

E-Mail karger@karger.com
www.karger.com/spp

Dr. Kerstin Reisinger
Henkel AG & Co. KGaA
Henkelstrasse 67
DE–40589 Düsseldorf (Germany)
E-Mail Kerstin.Reisinger@henkel.com

ror the human in vivo situation realistically for the species- and organ-specific safety assessment of dermally applied compounds regarding corrosion, irritation, genotoxicity and sensitization. 3D skin models offer the added advantage of being suitable for testing lipophilic compounds, which, due to their lack of water solubility, cannot be easily tested in monolayer cell cultures.

As a result, a growing number of skin models have been incorporated into in vitro genotoxicity and sensitization assays to improve their predictive capability. It is of importance to measure the levels of phase I and II enzymatic activities in skin models that are used in safety evaluation studies. Phase I enzymes such as cytochrome P450 (CYP) or flavin-dependent monooxygenases (FMOs) activate lipophilic compounds by introducing a polar group into the xenobiotic. The activated intermediates may be substrates of phase II enzymes, which conjugate the substrates to result in a more hydrophilic and excretable molecule. In contrast to the liver, less is known about the xenobiotic metabolism of the skin and appropriate in vitro systems and about how the activities are regulated. Although some studies have performed comprehensive gene expression analyses of xenobiotic metabolizing enzymes (XMEs) in native skin and 3D skin models [3, 8], only a few publications have investigated both enzyme gene expression and phase I and II activities in skin models.

We have prepared and analyzed 4 in vitro models of different physiological complexities (from monolayers to 3D) and compared them with native human skin. The models were: the Phenion® Full-Thickness (Phenion FT) Skin Model [9], the Open-Source Reconstructed Epidermis (OS-REp) model [10] and monolayer cultures of fibroblasts and keratinocytes.

The OS-REp model is a recently introduced 3D skin model for which the intellectual property and the tissue production protocol are available to everyone (hence 'open-source'). It is based on a serum-free and chemically defined tissue culture technique described by Poumay et al. [11] that allows the reconstruction of human epidermis from primary human keratinocytes, with the resulting tissue models exhibiting basic epidermal characteristics. The reproducibility of its production and the suitability of the tissue for predicting the skin irritation potential of products will be verified in a validation study.

The Phenion FT Skin Model consists of keratinocytes and fibroblasts forming an epidermis, a basement membrane and a dermis with a morphology and tissue functionality similar to those of native human skin [9, 12]. The barrier properties of this model appear to increase with the lipophilicity of the test compounds, confirming the additional reservoir or physical barrier formed by the dermis equivalent [12]. There is evidence that xenobiotic metabolism may be influenced by cross-talk between dermal fibroblasts and epidermal keratinocytes [13]. Therefore, it may be expected that the metabolic capacity of this model may be closer to native skin than that of 2D or 3D skin models which represent the epidermis only.

The aim of the present study was to investigate which dermal model best reflected the in vivo situation such that it may be used for safety assessment tests. To this end, we compared a number of phase I and phase II metabolic profiles in the epidermis and dermis of native human skin and the different skin models at the levels of gene expression as well as protein and enzymatic activity. All 4 skin models were compared with native skin from the same 3 human donors so that donor variation could be excluded from the comparisons. In order to achieve this, the first half of the skin sample was directly subjected to gene expression analysis, whereas cells from the second half were isolated and propagated as monolayer cultures of either keratinocytes or fibroblasts. Thereafter, OS-REp and Phenion FT Skin Models were prepared using cells from the same donors. To enable a comparison of the organ-specific assessment by skin models with the assessment by a hepatic model, HepG2 cells were chosen as a well characterized cell line with a reproducible culture method. These cells have been shown to exhibit phase I and II metabolizing activities if cultured under suitable conditions [14, 15]. In order to better compare the 3D skin models with the hepatic model, we also cultured the HepG2 cells in a 3D format, i.e. spheroids.

Methods

Chemicals

β-Naphthoflavone (β-NF), phenobarbital, all-*trans*-retinoic acid, 7-ethoxyresorufin, dicoumarol, 4-methylumbelliferone, collagenase and thermolysin were purchased from Sigma (Germany). All medium components and trypsin solution were purchased from Invitrogen (Darmstadt, Germany) unless stated otherwise.

Cell Isolation and Culture Medium

The human fibroblasts and keratinocytes used for each model were isolated from foreskin tissue, as described by Mewes et al. [9]. The dermis and epidermis were first separated by incubating in thermolysin overnight. After separation, the epidermal layer was then incubated in a trypsin solution until it was completely dissociated into a single cell suspension of keratinocytes. The connective tissue was dissociated and fibroblasts released by incubation in a solution containing 0.2 IU/ml collagenase. Fibroblasts were harvested and seeded in cell culture flasks in DMEM with GlutaMAX supplemented with 10% FCS (PAA

Laboratories, Cölbe, Germany), 1 mM ascorbic acid 2-phosphate (Sigma), 100 IU/ml penicillin and 100 μg/ml streptomycin. For comparison with the 2D cultures, keratinocytes were cultured in EpiLife medium (Cascade Biologics, Portland, Oreg., USA) containing HKGS supplemented with 1.5 mM $CaCl_2$ (Cascade Biologics).

For the preparation of 3D cultures, keratinocytes were seeded into cell culture flasks inoculated with feeder cells (mitomycin-inactivated fibroblasts in keratinocyte medium) in DMEM with GlutaMAX/Ham's F12 medium (3:1) supplemented with 10% Fetalclone II (HyClone, Logan, Utah, USA), cholera toxin, adenine, hydrocortisone, epidermal growth factor, insulin, triiodothyronine, ascorbic acid 2-phosphate (all from Sigma), 100 IU/ml penicillin and 100 μg/ml streptomycin. Organotypical skin models were prepared from fibroblasts up to a maximum passage of 5, and keratinocytes up to a maximum passage of 3.

Phenion FT Skin Model

Fibroblasts were first seeded onto the equilibrated collagen matrices in fibroblast growth medium at 3–5·10^5 cells per matrix for 2 weeks, during which time the culture medium was changed daily. Keratinocytes were seeded on top of the fibroblast-colonized matrix. The keratinocyte growth medium was changed daily. After 1 week of culture under submerged conditions, the developing skin models were then lifted to the air-liquid interphase (ALI) and further cultured in DMEM with GlutaMAX/Ham's F12 medium (3:1) supplemented with 1.6 mg/ml bovine serum albumin, 0.4 g/ml hydrocortisone, 0.12 IU/ml insulin, 1 mM ascorbic acid 2-phosphate (all from Sigma), 100 IU/ml penicillin and 100 μg/ml streptomycin. Analyses were started after culturing the models in ALI medium at the ALI for 12 days. For analysis, the dermal and epidermal layers from the Phenion FT Skin Model were separated by incubation with dispase for 3 h at 4°C. This enzyme was found to have a minimal effect on the expression of over 1,300 skin-relevant genes (using DNA chips; Miltenyi Biotec, Bergisch Gladbach, Germany).

Open-Source Reconstructed Epidermis

Keratinocytes were cultured at a high cell density (5·10^5 cells/cm^2) for 12 days in serum-free and high-calcium (1.5 mM) EpiLife medium (Cascade Biologics) on an inert polycarbonate membrane at the ALI [11].

HepG2 2D and 3D Cultures

For comparison with the monolayers, HepG2 cells were seeded at 2,000 cells/well in a 96-well plate in DMEM with GlutaMAX supplemented with 10% FCS (PAA Laboratories). For the preparation of spheroids, a methyl cellulose stock solution was prepared in phenol red-free DMEM according to Korff et al. [16]. The HepG2 cells were resuspended in 10 ml medium containing 20% methyl cellulose and seeded in 100 μl at 200 and 400 cells/well in a 96-well nonadhesive round-bottom tissue culture plate (Greiner, Frickenhausen, Germany). This method resulted in the formation of spheroids within 24 h, after which point the cells were characterized for XMEs. Hepatocyte function was also monitored by measuring two hepatic markers, albumin and urea. Albumin was measured by enzyme-linked immunosorbent assay (Albumin ELISA Kit; Assaypro, St. Charles, Mo., USA), and the urea content in the supernatant medium samples was quantified by colorimetric determination at 470 nm using the Urea Assay Kit by BioChain (Newark, Calif., USA). Both proteins were secreted by the spheroids over 24, 48 and 72 h at levels which were higher than in the monolayer cultures (data not shown).

Gene Expression Analysis

Total RNA was extracted from the native human skin, 3D models or cells using the RNeasy Kit (Qiagen, Hilden, Germany) according to the supplier's instructions. Two micrograms of total RNA were reverse-transcribed utilizing random primers for amplification (Promega) and the Omniscript®-RT Kit (Qiagen), following the manufacturer's protocol. Real-time PCR was performed using a Bio-Rad iCycler iQ detection system (Bio-Rad Laboratories, Munich, Germany) in combination with TaqMan gene expression assays (Applied Biosystems, Foster City, Calif., USA). Each kit for the genes of interest (online suppl. table S1; for all online suppl. material, see www.karger.com/doi/10.1159/000358272) contained gene-specific primers and fluorogenic probes that were preoptimized by the manufacturer to yield 100 ± 10% amplification efficiency using human tissue RNA pools. The real-time PCR reaction was carried out in Thermo-Fast plates (ABgene, Hamburg, Germany). The cycling conditions were the following: 50°C for 2 min (1 cycle), 95°C for 10 min (1 cycle), 95°C for 1 s and 60°C for 1 min (40 cycles). The ΔCt method was applied for the relative quantification of gene expression, and β-actin was used as a reference gene. Preliminary tests showed that β-actin was the most stable reference gene under test system conditions. For the calculation, we chose a conservative Ct value of 34. This cutoff was chosen because CYP3A4 mRNA was not detected at Ct values below 34 in samples which contained this CYP at the protein level (data not shown).

Western Blot Analysis

Cells were harvested in RIPA buffer (50 mM Tris/HCl, pH 7.5; 1 mM EDTA; 1% SDS; 150 mM NaCl). Twenty micrograms of total protein were subjected to SDS-PAGE on gradient gels (4–12.5%; Invitrogen). The separated proteins were transferred onto nitrocellulose membranes by electroblotting at 170 mA for 2 h. After blocking with 5% low-fat milk powder and incubation overnight at 4°C with the first antibody (1:1,000 CYP3A4 mouse polyclonal antibody; Abnova, Taipeh, Taiwan), the blots were further processed for chemiluminescence detection, using a second antibody (1:250 anti-mouse IgG-peroxidase conjugate; Sigma) for 2 h at room temperature and the ECL Plus Kit (Amersham Biosciences, Freiburg, Germany).

Enzyme Activities

For the determination of ethoxyresorufin O-deethylase (EROD) activity, intact epidermis (separated and thoroughly washed in PBS) or intact cells were incubated in 12-well plates with 1 μM 7-ethoxyresorufin in fresh phenol red-free medium supplemented with 25 μM dicoumarol. After separation of the epidermis from the dermis, it was practically only possible to measure resorufin-related activity in the intact epidermal part of the Phenion FT Skin model. Resorufin fluorescence was measured directly in 24-well plates. The change in fluorescence was measured over 40 min at 37°C at 530 nm excitation and 590 nm emission. Activities were expressed as the rate of change in relative fluorescence units (dRFU) per minute per microgram protein for the skin models and the rate of dRFU per minute per 100 cells for the HepG2 models.

Glutathione S-transferase (GST) activity was measured according to the protocol of Habig et al. [17], using the GST Assay Kit by Sigma (Germany). The cytosolic fraction was prepared by centrif-

Table 1. Basal gene expression profile in native human skin and different in vitro models

	Native human skin		Phenion FT Skin Model		OS-REp	Monolayers	
	dermis	epidermis	dermis	epidermis		fibroblasts	NHEKs
Phase I enzymes							
CYP1A1	+/–/+	++/–/++	–/–/–	–/–/–	++/++/++	+/+/+	+/+/+
CYP1B1	++/+++/+++	++/++/++	++/++/++	+/+/+	+++/+++/++	++/++/++	++/++/+
CYP2A6	–/–/+	–/–/++	–/+/+	–/+/–	+/+/+	–/–/+	–/–/–
CYP2B6	–/–/–	–/–/–	–/–/–	–/–/–	–/–/–	–/–/–	–/–/–
CYP2D6	–/–/–	–/–/–	–/–/–	–/+/–	+/+/+	–/–/–	–/+/+
CYP2E1	++/++/++	++/+++/+++	+/+/+	+/++/+	++/++/++	+/+/+	+/+/+
CYP2S1	++/++/++	++/+++/+++	+/+/+	++/+/++	+++/++/++	+/+/+	++/+/++
CYP3A4	–/+/–	++/++/++	–/–/+	–/+/–	++/+/+	–/–/–	–/–/–
FMO1	++/++/++	++/+++/+++	++/++/++	+/+/+	++/++/++	+/–/+	–/–/–
FMO3	+/++/++	–/–/–	+/+/+	–/–/–	–/–/–	+/+/+	–/–/–
FMO5	++/++/++	+++/+++/+++	+/+/+	++/+/+	+++/+++/++	+/+/+	+/+/+
Phase II enzymes							
NAT1	++/++/++	++/++/+++	+/+/+	++/+/+	+++/++/++	+/+/+	+/++/++
UGT1A10	++/++/++	+++/+++/+++	++/+/+	++/++/++	+++/+++/+++	–/–/–	++/++/++
GSTP1	+/++/++	++/+++/+++	++/++/++	+++/++/+++	+++/++/+++	++/++/++	++/++/++

Comparison of basal gene expression levels between 3 foreskins from males not older than 4 years and 4 different in vitro models made of the 3 appropriate foreskins to exclude donor variability. The order of donors in the different columns and lines is always donor 1/2/3. RNA isolation, cDNA translation and PCR were performed as described in the Methods section. ΔCt values are presented as follows: – 'not detected'; + 'ΔCt to β-actin control >10', i.e. weak gene expression; ++ 'ΔCt = 5–10', i.e. moderate gene expression, and +++ 'ΔCt <5', i.e. high gene expression. All results are based on duplicates.

ugation at 15,000 *g* for 15 min. CDNB (1-chloro-2,4-nitrobenzene) was used as a broad-spectrum substrate of GSTs. The time-dependent kinetics of conjugate formation in the cytosol was obtained using a 96-well plate reader set at 340 nm. The blank contained buffer instead of protein to detect nonenzymatic CDNB conjugation. The GST activities were expressed as nanomoles per minute per milligram protein for both the skin and HepG2 models.

UDP-glucuronyltransferase (UGT) activity was determined as described by Gomez-Lechon [18]. Briefly, 4-methylumbelliferone (100 μM final concentration) was incubated with the cultures for 1 h. Samples were diluted 1:20 in 10 mM NaOH, and the remaining 4-methylumbelliferone was quantified fluorometrically at 376 nm excitation and 460 nm emission. The values were calculated as micromolars of 4-methylumbelliferone consumed per minute per milligram protein for the skin models, and as micromolars of 4-methylumbelliferone consumed per minute per 100 cells for the HepG2 models.

Results

Comparison of Basal Gene Expression Profiles in Native Human Skin with That in the Four Donor-Linked in vitro Dermal Test Systems

The basal gene expression of the phase I and phase II enzymes in each model was compared with that in the native skin from which these models were derived (table 1). For most of the enzymes studied in the native human skin, there was some variability between donors, particularly with regard to CYP1A1, CYP2A6 and CYP3A4 expression, which – depending on the CYP – were present at marked levels in one donor but absent in another. In addition, the gene expression level of approximately 60% of the genes analyzed was higher in the epidermis than in the dermis. For example, CYP1A1, CYP2A6, CYP2E1, CYP2S1 and CYP3A4 showed a tendency to be more prominently expressed in the epidermis. The exception was CYP1B1, which was present at higher levels in the dermis. The levels of CYP2D6 and CYP2B6 in native human skin were below the limit of detection. The non-CYP phase I enzymes FMO1 and FMO5 were highly expressed in both the dermal and epidermal compartments, whereas FMO3 was only detected in the dermis of native human skin. The phase II enzymes N-acetyltransferase (NAT) 1, UGT1A10 and GSTp1 were all expressed at high levels in both compartments of the native skin from all 3 donors.

When comparing the results for the native human skin with those for the 4 in vitro systems, a clear picture

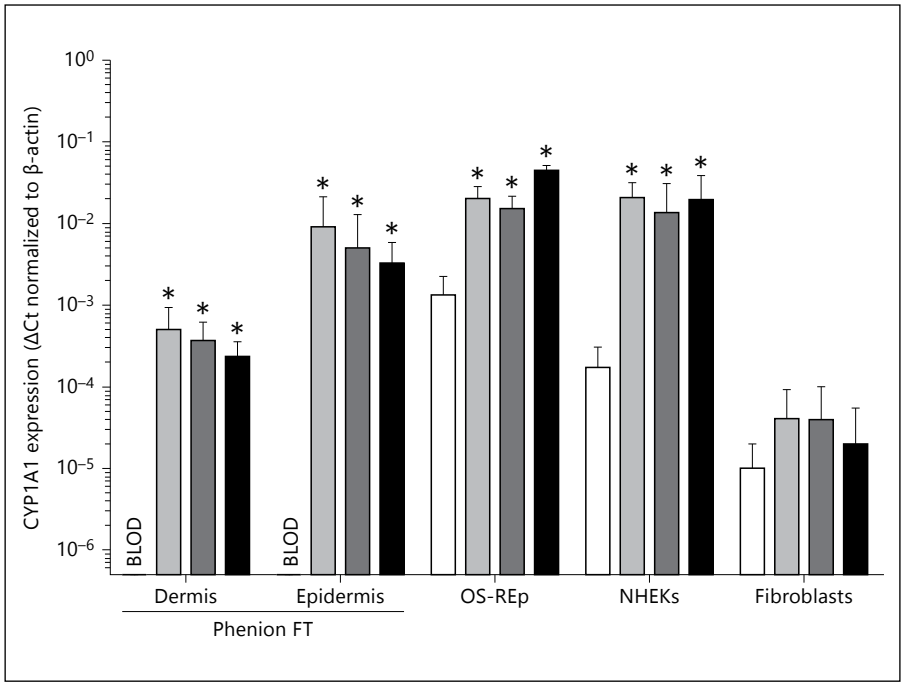

Fig. 1. Basal and β-NF induced CYP1A1 mRNA expression in different in vitro skin models. Skin models were constructed with cells from the same biopsy from 3 donors. Values denote means ± SD. * $p < 0.05$. White columns: solvent control; light gray columns: 24 h β-NF; dark gray columns: 48 h β-NF; black columns: 72 h β-NF. BLOD = Below the lower limit of detection.

becomes evident. A decreasing complexity of the test systems leads to a decrease in gene expression: CYP2A6, CYP3A4, FMO1 and UGT1A10 expression was below the detection limit in normal human epidermal keratinocytes (NHEKs) from all donors in the monolayer culture and clearly detectable in the more complex models. The only exception was CYP2D6, which was below the detection limit in native human skin but, if cultured in monolayers, was detected in the NHEKs from 2 of the 3 donors.

The expression of all the investigated enzymes in both compartments of the Phenion FT Skin Model was comparable with that in native skin, albeit at a marginally lower level. The exceptions to this were CYP1A1, which was present in the original donor but not in the Phenion FT Skin Model, and CYP2D6, which was expressed in the epidermis of 1 donor of Phenion FT Skin Model but not in the native skin of the same donor.

The constitutive expression of the enzymes in the epidermal model, OS-REp, compared well with that in the epidermal compartment of native skin. One notable exception was CYP2D6 expression in the OS-REp models of all donors, which was lacking in the native epidermis. Using Western blotting of CYP2D6, protein expression was also investigated in native skin and the Phenion FT Skin Model, but no protein was detected in either tissue (data not shown).

Comparison of Basal and Induced Levels of Phase I and II Enzymes in Skin with Those in the Liver Models

The 3D skin models were compared with the hepatic in vitro model using HepG2 cells. The importance of 3D culturing for differentiated phenotyping was investigated by using cells cultured as spheroids or in monolayers. To correlate the dermal test systems with a liver system, 3 representative groups of enzymes were chosen, which comprised 2 CYPs (CYP1A1 and CYP3A4), 1 non-CYP phase I enzyme (FMO3) and 2 representative phase II enzymes (UGT and GST).

CYP1A1

Figure 1 shows the basal gene expression of CYP1A1 in the different in vitro skin models, and because the values were reproducible across all 3 donors, the values shown are means of the 3 donors. The level of CYP1A1 mRNA was below the lower limit of detection in both the dermis and epidermis compartments of the Phenion FT Skin Model. CYP1A1 mRNA was detected in control-treated OS-REp and monolayers of NHEKs and fibroblasts, although the corresponding basal EROD activities were near to the limit of detection in all 4 skin models (fig. 1, 2). Despite the low basal mRNA expression of this CYP, it was readily inducible in intact Phenion FT Skin and OS-REp models and in monolayers of NHEKs by 25 μM β-NF over 72 h (fig. 1), an

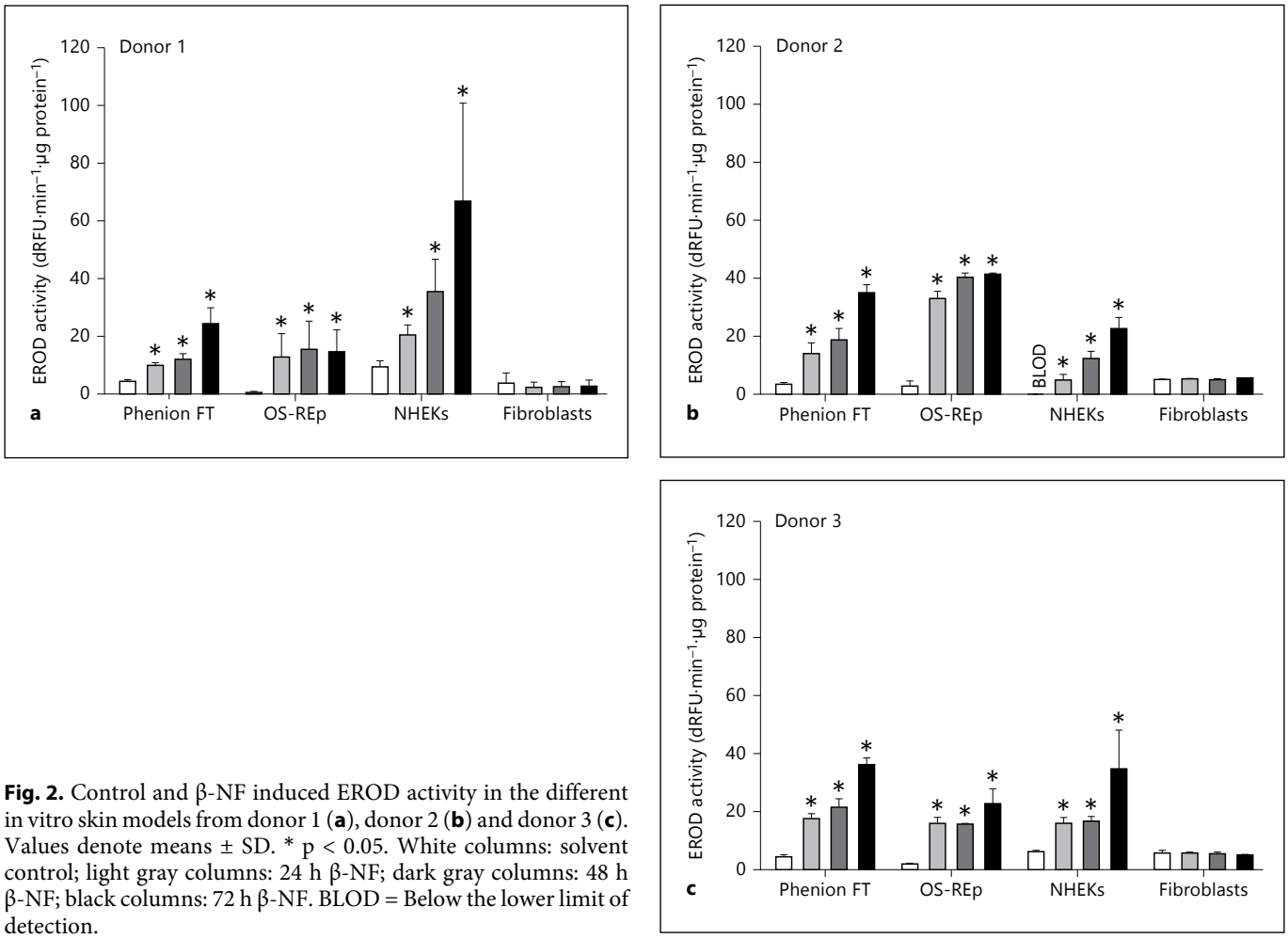

Fig. 2. Control and β-NF induced EROD activity in the different in vitro skin models from donor 1 (**a**), donor 2 (**b**) and donor 3 (**c**). Values denote means ± SD. * $p < 0.05$. White columns: solvent control; light gray columns: 24 h β-NF; dark gray columns: 48 h β-NF; black columns: 72 h β-NF. BLOD = Below the lower limit of detection.

effect that was maximal at 24 h. The increase in CYP1A1 mRNA expression was mirrored by an increase in EROD activity, although the relative levels of activity reached in β-NF-induced models were different as well as donor dependent. The highest induced activity was measured in keratinocyte cultures from donor 1 after 72 h of β-NF treatment (67 dRFU·min^{-1}·µg protein^{-1} vs. <45 dRFU·min^{-1}·µg protein^{-1} in other models from this donor and other treatments). In contrast to the other 3 models, CYP1A1 mRNA expression and EROD activities were not induced by β-NF in monolayer fibroblasts in any of the 3 donors at any time point over 72 h (fig. 1, 2). Notably, the EROD activities in fibroblast monolayers from all 3 donors were lower than in the corresponding NHEKs from the same donors. This was in line with the lack of EROD activity in the dermis of the Phenion FT Skin Model (data not shown).

CYP1A1 mRNA was constitutively expressed and induced in HepG2 3D spheroids by 25 µM β-NF over 72 h. CYP1A1 expression was induced by β-NF in spheroids with lower cell numbers (200 and 400 cells) but not in HepG2 cells cultured as monolayers (data not shown). The EROD activity in HepG2 cells was always higher when they were cultured as spheroids than when cultured as monolayers (fig. 3). The induction response of spheroids to β-NF was evident at 48 and 72 h. Although EROD was induced in monolayer cultures of HepG2, its activity remained low even if treated with β-NF (fig. 3).

CYP3A4

One of the most important drug-metabolizing enzymes in the liver is CYP3A4, and this was found to be constitutively expressed in the HepG2 cultures. Treatment with 2 mM phenobarbital caused no significant increase in CYP3A4 gene expression after 24 and 72 h in spheroids and in monolayers (data not shown). Native human skin was found to have only a low level of CYP3A4

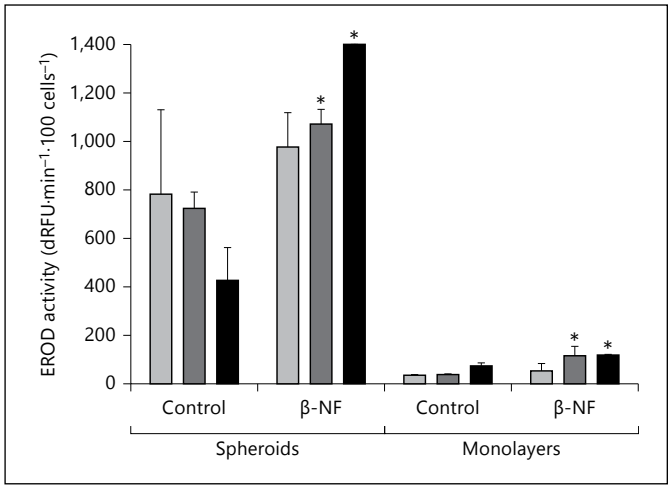

Fig. 3. Basal and induced EROD activity in HepG2 cells cultured as spheroids or monolayers. Values denote means ± SD. * $p < 0.05$. Each bar represents the mean ± 3 experiments. Light gray columns: 24 h β-NF; dark gray columns: 48 h β-NF; black columns: 72 h β-NF.

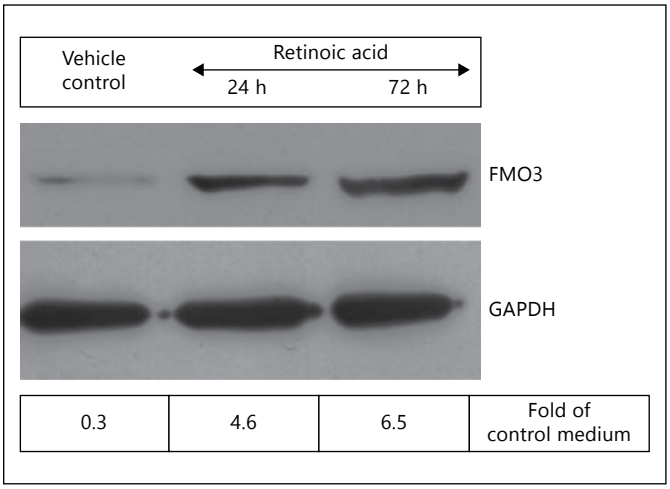

Fig. 4. Western blot analysis of FMO3 in native human skin. Ex vivo biopsies were incubated for 24 and 72 h with 10 μM all-*trans*-retinoic acid. Vehicle controls (ethanol) were conducted in parallel.

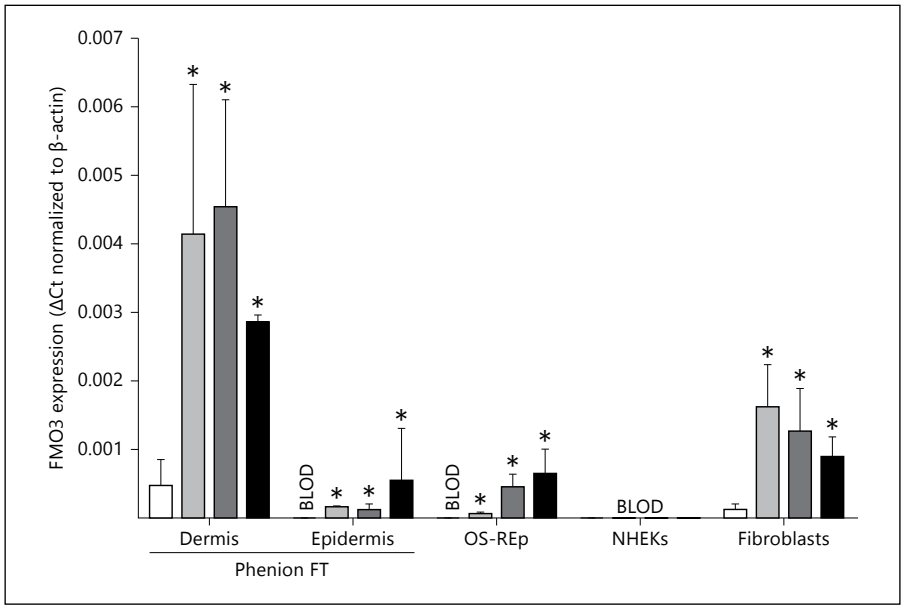

Fig. 5. FMO3 expression at the mRNA level induced by all-*trans*-retinoic acid in both compartments of the Phenion FT Skin Model, the OS-REp model and fibroblast monolayers. Values denote means ± SD. * $p < 0.05$. White columns: 0 h; light gray columns: 24 h; dark gray columns: 48 h; black columns: 72 h. BLOD = Below the lower limit of detection.

protein, moderately induced after 24 h by 2 mM phenobarbital (measured by Western blotting; data not shown). The level of induction was not further increased between 24 and 72 h. Despite the moderate increase in CYP2B6 mRNA, this did not result in an increase in CYP3A4-dependent BROD activity by phenobarbital (0.5–2 mM for 24, 48 and 72 h), rifampicin (50 and 100 μM for 24 h) or dexamethasone (10 and 50 μM for 24, 48 and 72 h).

Flavin-Dependent Monooxygenase 3

All-*trans*-retinoic acid, at a concentration of 10 μM, induced FMO3 in native human skin after 24 h, and this induction was sustained up to 72 h (measured by Western blot analysis; fig. 4). All-*trans*-retinoic acid also induced FMO3 at the mRNA level after 24 h in both compartments of the Phenion FT Skin Model, the OS-REp model and fibroblast monolayers (fig. 5). By contrast,

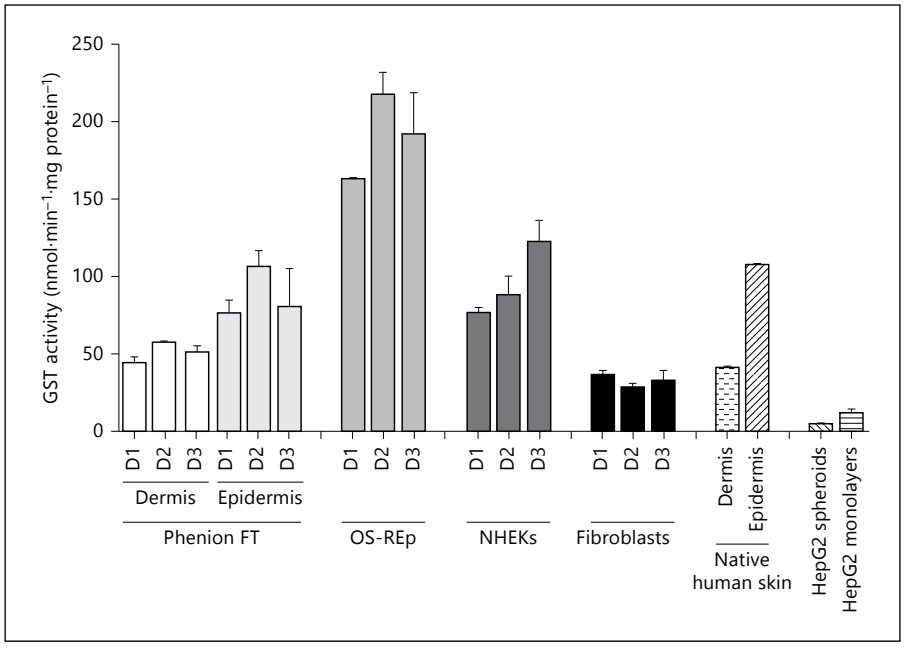

Fig. 6. GST activity in the in vitro skin models compared with that in native human skin and HepG2 cells. Values denote means ± SD. D1/2/3 = Donor 1/2/3.

FMO3 was not constitutively expressed or induced by all-*trans*-retinoic acid in NHEK cultures from any of the 3 donors. In contrast to native skin and the in vitro dermal models (table 1), FMO3 mRNA expression was below the limit of detection in HepG2 cells cultured as spheroids or monolayers.

Glutathione S-Transferase

GST activity in the in vitro skin models of variable complexity was compared with that in native human skin and HepG2 cells (fig. 6). GST activity in the native human skin from intact biopsies was 80 nmol·min^{-1}·mg protein^{-1}; it was present at higher levels in the epidermis (100 nmol·min^{-1}·mg protein^{-1}) than in the dermis (40 nmol·min^{-1}·mg protein^{-1}). The relative levels of GST activity in the epidermis and dermis of the Phenion FT Skin Model were comparable with those measured in the two compartments of native human skin. Likewise, GST activity was higher in NHEKs than in fibroblast monolayers. The highest GST activity was measured in the OS-REp model (160–220 nmol·min^{-1}·mg protein^{-1}), whereas fibroblasts showed the lowest GST activity.

There was no constitutive gene expression of the dermally located GST subtype p1 in HepG2 spheroids or monolayer cultures. However, a GST-mediated metabolism of CDNB was clearly measurable in HepG2 spheroids and monolayers (fig. 6). In contrast to CYP1A1 and CYP3A4 activities, GST activity was markedly lower in HepG2 cells (5–13 nmol·min^{-1}·µg protein^{-1}) than in any of the in vitro skin models tested.

UDP-Glucuronyltransferase

Basal UGT activity was measurable in all the in vitro models tested (fig. 7) and varied between 1 and 6 µM·min^{-1}·mg protein^{-1}. Despite the fact that the level of activity was donor dependent, it was always higher in the Phenion FT Skin Model than in the other models. The UGT activity in the Phenion FT Skin Model was marginally higher in the dermal than in the epidermal compartment. It was statistically significantly increased in the Phenion FT Skin Models from 2 donors (fig. 7a, c) and in fibroblasts from donor 3 (fig. 7c) after 72 h. By contrast, in the OS-REp model as well as in the NHEK and fibroblast monolayers, UGT activity was not induced by treatment with β-NF for up to 72 h.

UGT1A10 mRNA was expressed at basal levels in HepG2 spheroids and monolayer cultures, in which the UGT activity was higher in the spheroids than in the monolayer cultures (fig. 8). Its activity in the spheroids was constant over 72 h and readily induced by β-NF at all the time points tested (2.7-, 3.8- and 6.6-fold increase at 24, 48 and 72 h, respectively). The activity increased gradually over time if HepG2 cells were cultured as monolayers, and the effect of β-NF was lower than in the spheroids (0.8-, 1.9- and 1.3-fold increase at 24, 48 and 72 h, respectively; fig. 8).

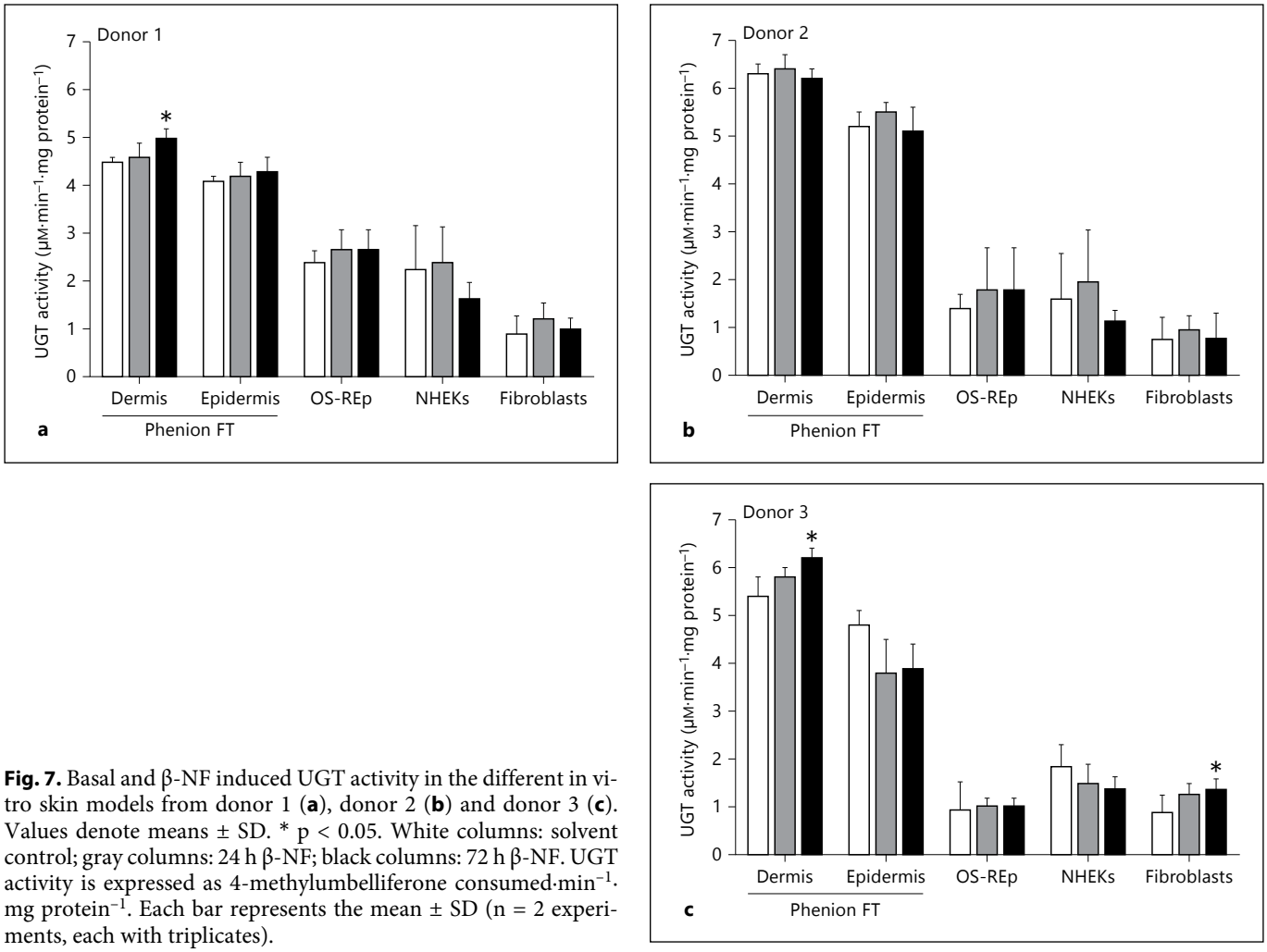

Fig. 7. Basal and β-NF induced UGT activity in the different in vitro skin models from donor 1 (**a**), donor 2 (**b**) and donor 3 (**c**). Values denote means ± SD. * $p < 0.05$. White columns: solvent control; gray columns: 24 h β-NF; black columns: 72 h β-NF. UGT activity is expressed as 4-methylumbelliferone consumed·min^{-1}·mg protein^{-1}. Each bar represents the mean ± SD (n = 2 experiments, each with triplicates).

Discussion

To perform risk assessments of chemicals that are dermally applied such as cosmetics, pharmaceuticals and agrochemicals, it is important to use relevant in vitro systems which mirror the human skin most realistically. Skin histology and barrier function of the commercially available skin models in particular are well known [19]. Several studies have been published regarding dermal xenobiotic metabolism [20–23]; however, a systematic analysis of test systems with different complexity is still lacking. Thus, the objective of our study was to close this gap and to characterize XMEs in in vitro models in order to interpret the results from skin sensitization and genotoxicity assays that use them.

A first approach, using semi-quantitative real-time PCR in combination with gene-specific TaqMan assays, showed that many hepatic enzymes which are involved in xenobiotic metabolism were also constitutively expressed in detectable quantities in native human skin; those were CYP1A1, CYP1B1, CYP2E1, CYP3A4, FMOs, GSTp1, UGT1A10 and NAT1. Most enzymes detected in both compartments of human native skin, were also expressed in both 3D skin models, with the exception of CYP1A1, which was lacking in the Phenion FT Skin Model. There are a number of reports of donor variation in the expression of CYPs (reviewed by Oesch et al. [2]), and this was also evident in our study with respect to CYP1A1, CYP2A6 and CYP3A4. Of the 3 donors tested here, none expressed CYP2B6. This is in accordance with results by Saeki et al. [24], wherein CYP2B6 expression was undetectable in different types of skin cell. Yengi et al. [25] reported a large range of CYP2B6 expression in native human skin from undetectable to high levels in some individuals.

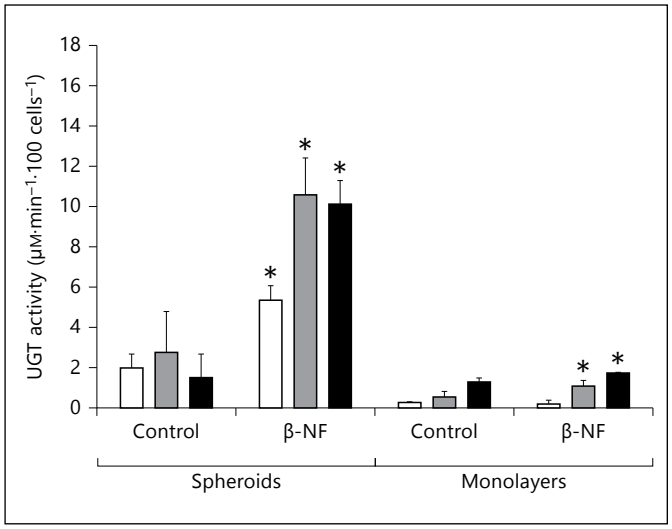

Fig. 8. UGT activities in HepG2 spheroids and monolayer cultures. Values denote means ± SD. * $p < 0.05$. White columns: solvent control; gray columns: 24 h β-NF; black columns: 72 h β-NF. UGT activity is expressed as 4-methylumbelliferone consumed·min^{-1}. mg protein^{-1}. Each bar represents the mean ± SD (n = 2 experiments, each with triplicates).

Likewise, there are reports that CYP3A4 is not expressed in whole human skin [3, 8], but this CYP was present at measurable levels in the epidermis of native skin from all 3 donors tested here. This expression was lost if the fibroblasts and keratinocytes were cultured as monolayers, but re-expressed in the 3D epidermal OS-REp model, suggesting a strong influence of the culture conditions. CYP2D6 expression was below the limit of detection in both compartments of native skin and the dermis of the Phenion FT Skin Model from all donors. However, a low expression was detected in the epidermis of the Phenion FT Skin Model from 1 donor, in the OS-REp model from all donors and in keratinocytes from 2 of the 3 donors. Since CYP2D6 is not inducible [26], the reason for the presence of this CYP in the 3D models and keratinocytes may lie in the fact that a higher concentration of keratinocytes was measured in the samples. In general, there was a lower basal gene expression of 10 (out of 13) enzymes in fibroblast and keratinocyte monolayer cultures than in native human skin; UGT1A10, for instance, was not detected in monolayer fibroblasts, and FMO1 was lacking in keratinocyte cultures from all 3 donors.

The dermis and epidermis of native human skin had distinct gene expression profiles. FMO3, for example, another phase I enzyme, was only detected in dermal compartments of both native human skin and the Phenion FT Skin Model, as well as in fibroblasts. Conversely, the OS-REp models and the keratinocytes from which they were derived lacked FMO3. This rather profound difference in FMO3 distribution is in accordance with the findings by Luu-The et al. [8]. FMO1, reported as being selectively expressed in the epidermis [8], was detected in the dermis of 2 of the 3 native skin donors in this study, as well as in the dermis of the Phenion FT Skin Model. Notably, FMO1 was absent from keratinocytes, but reexpressed if the keratinocytes were cultured as the 3D OS-REp model, suggesting this enzyme is strongly affected by the culture conditions [2].

Another example in which the relative expression of an enzyme was different is UGT1A10, an important phase II enzyme involved in the detoxification of polycyclic aromatic hydrocarbons [27] and in the metabolism of many compounds after dermal exposure [28]. The basal gene expression of this enzyme was higher in the epidermis than in the dermis of native skin and the Phenion FT Skin Model, was present at high levels in the OS-REp model, and was present at lower levels in NHEK cells but absent in fibroblasts. This suggests that UGT1A10 is mainly expressed in keratinocytes and may require a 3D environment with other cells to be expressed in fibroblasts.

Like UGTs, NAT1 is a well-described major detoxification enzyme in the skin, whereas NAT2 is not expressed in this organ. The basal gene expression levels of NAT1 were similar in the dermal and epidermal compartments of native skin and the Phenion FT Skin Model, and it was ubiquitously expressed in all in vitro models tested. This is in line with recent publications showing that the activity of NAT1 can be several-fold higher in the skin than in the liver [29] and can also be determined in a keratinocyte cell line such as HaCaT [30].

The inducibility of CYP1A1 in in vitro models of variable complexity was investigated using the prototypical inducer β-NF [31–33]. CYP1A1 gene expression was most strongly induced in the Phenion FT Skin Model and in NHEKs. CYP1A1 was also induced to a lower extent by β-NF in the OS-REp model; however, this epidermal model also expressed higher basal levels of CYP1A1 than did the other in vitro models. In fibroblasts, an induction of CYP1A1 gene expression was only observed if they were cultured in the Phenion FT Skin Model, not if they were cultured as monolayers, in which this enzyme was always present at low levels (as also observed by Sadek and Allen-Hoffmann [34]). EROD activities, reflecting CYP1A1-, CYP1A2- and CYP1B1-mediated metabolism [35], were generally at the limit of detection in all in vitro skin models and much lower than in HepG2 cells. The

only exception to this was the EROD activity in NHEKs from 2 of the 3 donors, which may have been increased by the growth factors in the medium. Others have also reported low or no basal EROD activity in dermal models [36, 37]. Treatment with β-NF resulted in a clear increase in EROD activities measured in HepG2 cells and in the intact epidermal compartment of Phenion FT skin and the OS-REp model, as well as in NHEKs from all 3 donors over time. Only fibroblast monolayers failed to respond to induction by β-NF. The low basal level of CYP1A1 expression in fibroblasts and the lack of induction of its expression or of EROD activity are in line with a report that the CYP1A1 protein is mainly localized in the epidermis [38].

The inducibility of CYP3A4 was analyzed using the prototypical inducer phenobarbital [39, 40]. Gene and protein expression analysis showed no inducibility of dermal CYP3A4 after systemic incubation for up to 72 h. Further investigations into the induction of various metabolic enzymes by different compounds included retinoic acid, which is a known inducer [41]. In our study, retinoic acid also induced FMO3 protein and mRNA expression in fibroblasts. Interestingly, FMO3 was also inducible in the epidermis of the Phenion FT Skin Model and the epidermal OS-REp model, which were shown to lack any basal gene expression of this enzyme. FMO3 induction could only be detected in the 3D models but not in the 2D keratinocyte model, suggesting more complex culture conditions are required for this process. To our knowledge, this is the first report of FMO3 being inducible by retinoic acid in dermal models.

GSTs are a supergene family of widely distributed isoenzymes which are essential for many conjugation reactions [42]. A number of isoforms of GST1 (alpha, mu and pi) have been identified in human skin, of which the GSTpi family, which is encoded by the GSTP1 gene, is the predominant form [42]. GSTpi is not inducible in skin by prototypical aryl hydrocarbon receptor (AhR)-mediated inducers [33, 43]; therefore, we focused on basal GST activity only. The GST activity in whole native human skin was higher in the epidermal compartment than in the dermal compartment, and this ratio of activity levels between the compartments was reflected in the Phenion FT Skin Model. The OS-REp model had the highest GST activity, which is in accordance with Harris et al. [33] and Luu-The et al. [8], who found that GST activities in reconstructed 3D epidermal models were equal or higher than the activity in the epidermal compartment of native human skin. Likewise, NHEKs also exhibited a generally high GST activity compared with native skin. These data demonstrate that both the dermis and epidermis are able to undergo glutathione conjugation.

Like GST activity, the basal activity of UGT, the second phase II enzyme selected for more in-depth analysis, was readily detectable in all 4 in vitro models. Interestingly, the highest activity was measured in the Phenion FT Skin Model. In addition, the activity was marginally higher in the dermal than in the epidermal compartment, despite the fact that the gene expression of this enzyme was higher in the epidermal compartment of this model. Protein levels of the UGT enzyme in cultured human keratinocytes have been reported to be induced by AhR agonists [44]; however, in our study, this activity was only marginally induced by β-NF (1.11-fold) after 72 h in the Phenion FT Skin Models from 2 donors and in fibroblasts from 1 donor (1.5-fold). The low mRNA expression of UGT1A10 in fibroblasts was reflected in the low rate of 4-methylumbelliferone metabolism. As with EROD activity, UGT activity was also not induced in fibroblasts, suggesting that these cells lack AhR responses.

A number of XMEs were selected to compare the metabolic capacity of the in vitro skin models with that of a hepatic model, i.e. HepG2 cells. In general, there was a higher expression of phase II enzymes than of phase I enzymes in the skin models. The CYP1A1 expression and activity were very low in the skin models, but CYP1A1 was clearly expressed in the hepatic model; moreover, EROD activity was several thousand-fold higher in the HepG2 cells than in the skin models (taking into account the protein content of HepG2 cells of 0.55 mg/1,000,000 cells [45]). CYP1A1 mRNA expression was induced by β-NF in the 2 in vitro 3D reconstructed skin models and in keratinocytes. Likewise, CYP1A1 expression and EROD activity were induced by β-NF in HepG2 cells, but only if cultured as spheroids, emphasizing the need for a 3D environment for optimal function. Unlike in the 3D in vitro skin models and fibroblasts, FMO3 was not upregulated by retinoic acid in spheroids or monolayer cultures of HepG2 cells.

UGT activity was also higher in HepG2 cells than in the skin models, since this activity could be readily detected in cultures of only 100 cells. UGT expression and activity were also shown to be readily inducible in the hepatic model, whereas in the in vitro skin models, this enzyme was only moderately induced, possibly due to the already high basal activity. Conversely, GST was expressed in the skin models, and its activity there was at least 2-fold higher than in the liver model. CYP1A1, CYP2D6, CYP3A4 and UGT1A10 were all present in

HepG2 spheroids and monolayers, but unlike in the skin models, the gene expression levels of FMO3 and GSTp1 were below the limit of detection in the HepG2 spheroids. This was expected in the case of GSTpi, which, despite being the most widely distributed enzyme of all GSTs and the most abundant form in many tissues, is not a major GST in the adult human liver but rather in the fetal liver [46]. FMO3 is the most abundant FMO isoform in the human liver [46], and we would have expected to have detected this in the HepG2 model.

In summary, the in vitro skin models showed distinctive profiles at the levels of gene expression and enzymatic activity with regard to xenobiotic metabolism. Organotypic models offer a way to construct a system which mirrors the in vivo situation more realistically than do monolayer cultures of either keratinocytes or fibroblasts. The differences between the test systems were more prominent than was donor variability. Furthermore, the differences between the compartments of either the native skin or the Phenion FT Skin Model were also greater than was the donor variability. Consequently, skin models seem to have a metabolic capacity close to the human in vivo situation. A comparison of phase I and phase II metabolism between in vitro dermal and hepatic models indicates that the bioactivation processes linked to phase I enzymes are more prominent in hepatic models and that detoxification activities mediated by phase II enzymes are more prominent in dermal models. These data support the use of 3D reconstructed human skin tissues as valuable test systems for improved in vitro assays in the fields of genotoxicity and sensitization research [47–49].

Disclosure Statement

The authors have no conflicts of interest.

References

1 Ahmad N, Mukhtar H: Cytochrome P450: a target for drug development for skin diseases. J Invest Dermatol 2004;123:417–425.
2 Oesch F, Fabian E, Oesch-Bartlomowicz B, Werner C, Landsiedel R: Drug-metabolizing enzymes in the skin of man, rat, and pig. Drug Metab Rev 2007;39:659–698.
3 Hu T, Khambatta ZS, Hayden PJ, Bolmarcich J, Binder RL, Robinson MK, Carr GJ, Tiesman JP, Jarrold BB, Osborne R, Reichling TD, Nemeth ST, Aardema MJ: Xenobiotic metabolism gene expression in the EpiDerm in vitro 3D human epidermis model compared to human skin. Toxicol In Vitro 2010;24:1450–1463.
4 Roguet R: The use of standardized human skin models for cutaneous pharmacotoxicology studies. Skin Pharmacol Appl Skin Physiol 2002;15:1–3.
5 Curren RD, Mun GC, Gibson DP, Aardema MJ: Development of a method for assessing micronucleus induction in a 3D human skin model (EpiDerm). Mutat Res 2006;607:192–204.
6 Directive 2003/15/EC of the European Parliament and of the Council of 27 February 2003 amending Council Directive 76/768/EEC on the approximation of the laws of the Member States relating to cosmetic products. Official Journal L66, 11/03/2003, p 26.
7 http://ec.europa.eu/environment/chemicals/reach/reach_intro.htm.
8 Luu-The V, Duche D, Ferraris C, Meunier JR, Leclaire J, Labrie F: Expression profiles of phases 1 and 2 metabolizing enzymes in human skin and the reconstructed skin models Episkin and full thickness model from Episkin. J Steroid Biochem Mol Biol 2009;116:178–186.
9 Mewes KR, Raus M, Bernd A, Zöller NN, Sättler A, Graf R: Elastin expression in a newly developed full-thickness skin equivalent. Skin Pharmacol Physiol 2007;20:85–95.
10 Heymer A, Schober L, Walter M, Traube A, Brode T, Drescher T, Fischer A, Reisinger K, Petersohn D, Mewes KR: The open source concept: shaping the future of animal-free tests (poster). DECHEMA Society for Chemical Engineering and Biotechnology Conference, Zurich, 2012.
11 Poumay Y, Dupont F, Marcoux S, Leclercq-Smekens M, Hérin M, Coquette A: A simple reconstructed human epidermis: preparation of the culture model and utilization in in vitro studies. Arch Dermatol Res 2004;296:203–211.
12 Ackermann K, Borgia SL, Korting HC, Mewes KR, Schäfer-Korting M: The Phenion® full-thickness skin model for percutaneous absorption testing. Skin Pharmacol Physiol 2010;23:105–112.
13 Stinchcomb AL: Xenobiotic bioconversion in human epidermis models. Pharm Res 2003; 20:1113–1118.
14 Westerink WM, Schoonen WG: Cytochrome P450 enzyme levels in HepG2 cells and cryopreserved primary human hepatocytes and their induction in HepG2 cells. Toxicol In Vitro 2007;21:1581–1591.
15 Westerink WM, Schoonen WG: Phase II enzyme levels in HepG2 cells and cryopreserved primary human hepatocytes and their induction in HepG2 cells. Toxicol In Vitro 2007;21: 1592–1602.
16 Korff T, Krauss T, Augustin HG: Three-dimensional spheroidal culture of cytotrophoblast cells mimics the phenotype and differentiation of cytotrophoblasts from normal and preeclamptic pregnancies. Exp Cell Res 2004; 297:415–423.
17 Habig WH, Pabst MJ, Jakoby WB: Glutathione S-transferase: the first enzymatic step in mercapturic acid formation. J Biol Chem 1974;249:7130–7139.
18 Gomez-Lechon MJ: Isolation, culture and use of human hepatocytes; in Castell JV (ed): Drug Research in in vitro Methods in Pharmaceutical Research, ed 1. San Diego, Academic Press, 1997.
19 Netzlaff F, Lehr CM, Wertz PW, Schaefer UF: The human epidermis models EpiSkin, SkinEthic and EpiDerm: an evaluation of morphology and their suitability for testing phototoxicity, irritancy, corrosivity, and substance transport. Eur J Pharm Biopharm 2005;60:167–178.
20 Neis MM, Wendel A, Wiederholt T, Marquardt Y, Joussen S, Baron JM, Merk HF: Expression and induction of cytochrome P450 isoenzymes in human skin equivalents. Skin Pharmacol Physiol 2010;23:29–39.
21 Baron JM, Höller D, Schiffer R, Frankenberg S, Neis M, Merk HF, Jugert FK: Expression of multiple cytochrome P450 enzymes and multidrug resistance-associated transport proteins in human skin keratinocytes. J Invest Dermatol 2001;116:541–548.
22 Du L, Neis MM, Ladd PA, Lanza DL, Yost GS, Keeney DS: Effects of the differentiated keratinocyte phenotype on expression levels of CYP1–4 family genes in human skin cells. Toxicol Appl Pharmacol 2006;213:135–144.
23 Hewitt NJ, Edwards RJ, Fritsche E, Goebel C, Aeby P, Scheel J, Reisinger K, Ouédraogo G, Duche D, Eilstein J, Latil A, Kenny J, Moore C, Kuehnl J, Barroso J, Fautz R, Pfuhler S: Use of human in vitro skin models for accurate and ethical risk assessment: metabolic considerations. Toxicol Sci 2013;133:209–217.

24 Saeki M, Saito Y, Nagano M, Teshima R, Ozawa S, Sawada J: mRNA expression of multiple cytochrome P450 isozymes in four types of cultured skin cells. Int Arch Allergy Immunol 2002;27:333–336.
25 Yengi LG, Xiang Q, Pan J, Scatina J, Kao J, Ball SE, Fruncillo R, Ferron G, Wolf CR: Quantitation of cytochrome P450 mRNA levels in human skin. Anal Biochem 2003;316:103–110.
26 Hewitt NJ, Lecluyse EL, Ferguson SS: Induction of hepatic cytochrome P450 enzymes: methods, mechanisms, recommendations, and in vitro-in vivo correlations. Xenobiotica 2007;37:1196–1224.
27 Dellinger RW, Fang JL, Chen G, Weinberg R, Lazarus P: Importance of UDP-glucuronosyltransferase 1A10 (UGT1A10) in the detoxification of polycyclic aromatic hydrocarbons: decreased glucuronidative activity of the UGT1A10^{139Lys} isoform. Drug Metab Dispos 2006;34:943–949.
28 Moss T, Howes D, Williams FM: Percutaneous penetration and dermal metabolism of triclosan (2,4,4′-trichloro-2′-hydroxydiphenyl ether). Food Chem Toxicol 2000;38:361–370.
29 Kawakubo Y, Yamazoe Y, Kato R, Nishikawa T: High capacity of human skin for N-acetylation of arylamines. Skin Pharmacol 1990;3:180–185.
30 Goebel C, Hewitt NJ, Kunze G, Wenker M, Hein DW, Beck H, Skare J: Skin metabolism of aminophenols: human keratinocytes as a suitable in vitro model to qualitatively predict the dermal transformation of 4-amino-2-hydroxytoluene in vivo. Toxicol Appl Pharmacol 2009;235:114–123.
31 Khan IU, Bickers DR, Haqqi TM, Mukhtar H: Induction of CYP1A1 mRNA in rat epidermis and cultured human epidermal keratinocytes by benz(a)anthracene and beta-naphthoflavone. Drug Metab Dispos 1992;20:620–624.
32 Gelardi A, Morini F, Dusatti F, Penco S, Ferro M: Induction by xenobiotics of phase I and phase II enzyme activities in the human keratinocyte cell line NCTC 2544. Toxicol In Vitro 2001;15:701–711.
33 Harris IR, Siefken W, Beck-Oldach K, Brandt M, Wittern KP, Pollet D: Comparison of activities dependent on glutathione S-transferase and cytochrome P-450 IA1 in cultured keratinocytes and reconstructed epidermal models. Skin Pharmacol Appl Skin Physiol 2002;15:59–67.
34 Sadek CM, Allen-Hoffmann BL: Cytochrome P450IA1 is rapidly induced in normal human keratinocytes in the absence of xenobiotics. J Biol Chem 1994;269:16067–16074.
35 Chang TK, Waxman DJ: Enzymatic analysis of cDNA-expressed human CYP1A1, CYP1A2, and CYP1B1 with 7-ethoxyresorufin as substrate. Methods Mol Biol 2006;320:85–90.
36 Rolsted K, Kissmeyer AM, Rist GM, Hansen SH: Evaluation of cytochrome P450 activity in vitro, using dermal and hepatic microsomes from four species and two keratinocyte cell lines in culture. Arch Dermatol Res 2000;300:11–18.
37 Bonifas J, Hennen J, Dierolf D, Kalmes M, Blömeke B: Evaluation of cytochrome P450 1 (CYP1) and N-acetyltransferase 1 (NAT1) activities in HaCaT cells: implications for the development of in vitro techniques for predictive testing of contact sensitizers. Toxicol In Vitro 2010;24:973–980.
38 Katiyar SK, Matsui MS, Mukhtar H: Ultraviolet-B exposure of human skin induces cytochromes P450 1A1 and 1B1. J Invest Dermatol 2000;114:328–333.
39 Luo G, Cunningham M, Kim S, Burn T, Lin J, Sinz M, Hamilton G, Rizzo C, Jolley S, Gilbert D, Downey A, Mudra D, Graham R, Carroll K, Xie J, Madan A, Parkinson A, Christ D, Selling B, LeCluyse E, Gan LS: CYP3A4 induction by drugs: correlation between a pregnane X receptor reporter gene assay and CYP3A4 expression in human hepatocytes. Drug Metab Dispos 2002;30:795–804.
40 Richert L, Abadie C, Bonet A, Heyd B, Mantion G, Alexandre E, Bachellier P, Kingston S, Pattenden C, Illouz S, Dennison A, Hoffmann S, Coecke S: Inter-laboratory evaluation of the response of primary human hepatocyte cultures to model CYP inducers: a European Centre for Validation of Alternative Methods (ECVAM)-funded pre-validation study. Toxicol In Vitro 2010;24:335–345.
41 Heise R, Mey J, Neis MM, Marquardt Y, Joussen S, Ott H, Wiederholt T, Kurschat P, Megahed M, Bickers DR, Merk HF, Baron JM: Skin retinoid concentrations are modulated by CYP26AI expression restricted to basal keratinocytes in normal human skin and differentiated 3D skin models. J Invest Dermatol 2006;26:2473–2480.
42 Raza H, Awasthi YC, Zaim MT, Eckert RL, Mukhtar H: Glutathione S-transferases in human and rodent skin: multiple forms and species specific expression. J Invest Dermatol 1991;96:463–467.
43 Vessey DA, Lee KH, Boyer TD: Differentiation-induced enhancement of the ability of cultured human keratinocytes to suppress oxidative stress. J Invest Dermatol 1995;104:355–358.
44 Vecchini F, Mace K, Magdalou J, Mahe Y, Bernard BA, Shroot B: Constitutive and inducible expression of drug metabolizing enzymes in cultured human keratinocytes. Br J Dermatol 1995;132:14–21.
45 Guo W, Huang N, Cai J, Xie W, Hamilton JA: Fatty acid transport and metabolism in HepG2 cells. Am J Physiol Gastrointest Liver Physiol 2006;290:G528–G534.
46 Haining RL, Hunter AP, Sadeque AJ, Philpot RM, Rettie AE: Baculovirus-mediated expression and purification of human FMO3: catalytic, immunochemical, and structural characterization. Drug Metab Dispos 1997;25:790–797.
47 Aardema MJ, Barnett BC, Khambatta Z, Reisinger K, Ouedraogo-Arras G, Faquet B, Ginestet AC, Mun GC, Dahl EL, Hewitt NJ, Corvi R, Curren RD: International prevalidation studies of the EpiDerm 3D human reconstructed skin micronucleus (RSMN) assay: transferability and reproducibility. Mutat Res 2010;701:123–131.
48 Aardema MJ, Barnett BB, Mun GC, Dahl EL, Curren RD, Hewitt NJ, Pfuhler S: Evaluation of chemicals requiring metabolic activation in the EpiDerm™ 3D human reconstructed skin micronucleus (RSMN) assay. Mutat Res 2012;750:40–49.
49 Pfuhler S, Bartel M, Blatz V, Brinkmann J, Downs TR, Engels U, Fischer A, Henkler F, Jeschke S, Krul C, Liebsch M, Pirow R, Reus A, Schulz M, Reisinger K: 3D Skin Comet assay validation using full thickness tissues: update on the ongoing validation. 11th Int Conf Environ Mutagens, Foz do Iguassu, 2013.